

Quantum dot phosphors $\text{CaS}:\text{Ce}^{3+}$ and $\text{CaS}:\text{Pb}^{2+}$, Mn^{2+} for improvements of white light-emitting diodes optic characteristics

Dieu An Nguyen Thi¹, My Hanh Nguyen Thi², Phuc Dang Huu³

¹Faculty of Electrical Engineering Technology, Industrial University of Ho Chi Minh City, Ho Chi Minh City, Vietnam

²Faculty of Mechanical Engineering, Industrial University of Ho Chi Minh City, Ho Chi Minh City, Vietnam

³Institute of Applied Technology, Thu Dau Mot University, Binh Duong Province, Ho Chi Minh City, Vietnam

Article Info

Article history:

Received May 19, 2021

Revised May 25, 2022

Accepted Jun 9, 2022

Keywords:

Color rendered rate

Dual-layer phosphorus

Luminescent efficiency

Mie-scattering theory

Remote-phosphor

Triple-layer phosphorus

ABSTRACT

The goal of this study is to discover a new method that uses standard phosphors and quantum dots to improve the lighting qualities and heat manipulation of white light-emitting diodes (WLEDs). Despite the popularity as a good ingredient that offers good color rendering properties, quantum dots (QDs) have not been widely employed in the fabrication of WLEDs, particularly, the utilization of QDs-phosphor-mixed nanocomposite is limited. We propose a unique packaging design based on the research's experimental findings. The layer of nanocomposites consisting of QDs and phosphors is horizontally positioned to the WLED for optimal lighting and heating efficiency. This study simulated and used four distinguishing white LEDs forms: mono-layer phosphorus, two double-layer remote phosphors featuring yellowish-red and yellowish-green organizations, and a triple-layer phosphor. In terms of color rendering and luminous outputs, the triple-layer phosphor configuration outperforms the other implementations, as per the finding.

This is an open access article under the [CC BY-SA](https://creativecommons.org/licenses/by-sa/4.0/) license.



Corresponding Author:

Phuc Dang Huu

Institute of Applied Technology, Thu Dau Mot University

No. 6, Tran Van On Street, Thu Dau Mot city, Binh Duong province, Vietnam

Email: danghuuphuc@tdmu.edu.vn

1. INTRODUCTION

White-colored light-emitted diodes (WLEDs) are a new light source with various advantages, including energy savings, high efficiency, and environmental friendliness. It has been emerged to be potential alternatives to traditional illumination sources of everyday lighting, from industrial and commercial to transportation and exhibition lightings [1]–[3]. The most common technique for fabricating WLEDs is to combine a GaN LED's chip with a $\text{Y}_3\text{Al}_5\text{O}_{12}:\text{Ce}^{3+}$ (YAG: Ce^{3+}) yellow phosphor, and then the two emitted blue and yellow lights converge to produce white lights. Despite its advantages, this technique lacks red-light elements to produce better color performance because the yellow phosphors fail to achieve red-light emission [4]. It lowers the color rendering index (CRI) and makes QDs-phosphor nanocomposites WLEDs more difficult to utilize. Since obviously increasing the red-light components is a great way to improve color-rendering properties, various red-phosphor types were combined with this yellow phosphor material to form a phosphorus layer. The deep red-phosphor type emits substantial light wavelength over 650 nm, which is beyond the perceptual range of human eyes, and thus the luminous quality is compromised [5]–[8]. Colloidal quantum dots (QDs) were therefore used as a substitute for conventional materials to produce color lights. Desired traits of relatively low emission spectra and high absorption spectra demand a lot of

improvements from QDs to address the deficiencies of previous materials [9]–[12]. Thanks to extensive researches, CdSe, InP, CuInS₂, C, CH₃NH₃PbBr₃, CsPbBr₃, and a variety of other QDs have aroused a lot of interest. CdSe QDs, a semiconductor that appears to be the most efficient compared to other QD kinds, and offers a great economic profit, are found in sections II–VI. The reason is that they possess the superb quantum performance of more than 95%, the fulfilled width at half of maximum (FWHM) in 20–30 nm, as well as the ability to change particle sizes for accommodating the whole intellectual spectra. The very first WLED applying QDs in the market created with CdSe QDs was an analyzed focus of researchers [13], [14]. Despite the widespread use of CdSe QD-WLEDs in applications ranging from general to advanced illumination, their ability was limited by the presence of Cd, a hazardous material to humans [15]. A lot of studies intensively proposed approaches to abolish the Cd element and determine the optimum alternatives; consequently, InP, CuInS₂, and carbon QDs had been by far the most potential candidates for solving this problem. Yet, the disadvantages of InP and CuInS₂ QDs were presented by their lower efficacy and wider FWHM than those of CdSe QDs; meanwhile, carbon QDs were ineffective at transforming long wavelength colors like red emitted light [16]–[18]. Because of their high luminescence quality and outstanding chromatic efficiency, particularly green [19], perovskite QDs such as CH₃NH₃PbBr₃ and CsPbBr₃ have been introduced to be new materials to achieve better color conversion. After considering all materials listed above, CdSe QDs appear to be the best option for enhancing the color rendering capacity of WLEDs.

Many QD-WLED packages have presented high compatibility during long operation hours with a remote phosphor setup. This setup gets the layer of QDs composite separated from the LED chip with a sufficient gap, which allows the package to yield greater quantum performance, and higher heating consistency [20]. The layer of phosphor particles mixed with QDs plays a role as a light-converting layer, however, confronts several drawbacks of inadequate energy-transfer quality, poor lighting efficacy, and high heat output because of the backward-scattered occurrences among QDs and phosphors [21]. Thus, the separation between these two composites could improve the overall performance of WLEDs. The phosphor layer and the QDs plate were separated and vertically arranged to solve this problem and boost WLEDs' optical and thermal efficiencies [22], [23]. In mixed-type WLEDs, the vertical packaging layout is applied; thus, as indicated by the increase in phosphor quantum yield in comparison with QDs, if the phosphorus sheet is placed adjacent to the LED chip [24]–[26], the phosphorus-layer order can initiate a direct impact on the WLED outputs. Besides, the phosphor or QDs' film close to the blue chip also influences the effectiveness of the color conversion process. When drawing a comparison in both cases, WLED using QDs-upon-phosphorus structure performs excellent luminescent efficiency (LE), CRI, and regulates heating efficiency. While the mixed-kind or phosphorus-in-QDs promotes QDs-within-phosphor as the best option for producing high-quality WLEDs. Though these WLED structures are advantageous in several ways, it is unable to suppress the reabsorption because of the green- and yellow-light absorptions induced by the red QDs as these phosphor-emitting lights pass through them. Besides, LEDs have a Lambertian intensity distribution, indicating that the efficacy of its energy transfer is inconsistent, and the intensity concentrates in the middle before eventually fading out to the sides. The solution to reabsorption and unevenly converted energy in this study is a horizontally layered packaging method. For the first time, the idea foundation of positioning QDs-phosphor composite films in horizontal order to enhance the lighting features of WLEDs is presented and studied. The WLEDs with four structural designs utilizing the remote phosphor concept are included in the research. They are mono-layer, double-layer featuring yellowish-red and yellowish-green phosphorus arrangements, and three-layer remote phosphorus configurations are placed as well as used by the studies to ensure this research's accuracy.

2. EXPERIMENTING AND SIMULATING PROCESS

2.1. Compositions of the phosphorus samples

In this study, we mainly use two phosphors: CaS:Pb²⁺, Mn²⁺, and CaS:Ce³⁺. It must ensure that the composition preparation of CaS:Pb²⁺, Mn²⁺ following Table 1. To begin, combine the CaCO₃ and MnCO₃ in a mixing bowl. Then heat the mixture in uncovered quartzite boats with H₂S under 1100 °C in an hour. Later pulverized it. Secondly, combine PbO, NH₄Cl with approximately 2–3 g of S (sulfur). After that, get them fired in capped quartz tubes with N₂ under 1,200 °C for 1 hour, and continue to grind it. It should be ground before being put in a tightly sealed container. In contrast to CaS:Mn²⁺ without Pb, the emission color of the product should be red-orange. The result should also have the emission peak at 2.04 eV, 0.28 eV as width (FWHM), and UV excitation efficiency show ++(48 eV), +(3.40 eV).

Next, keep the number of ingredients listed in Table 2 when preparing the CaS:Ce³⁺. To begin, thoroughly combine all components. For the first 1 hour, heat the mixture with N₂, and another hour with H₂S in open quartz boats. Afterward, powder it and allow roughly 1–2 g of Ammonium chloride (NH₄Cl) to pass through by powdering or milling. Then, for 1 hour, fire them in capped quartz tubes with N₂ under 1,200 °C. Eventually, grind it into a powder. Finally, put it in a tightly sealed bottle. The emission color

should be green and the emission peak at 2.13 eV, 2.38 eV. The end outcome should also include the following characteristics: UV-excited efficacy is ++(4.88 eV)-(3.40 eV); e-beam excited efficacy is ++/20%. It has to be a microsecond-scale non-hyperbolic deterioration. Furthermore, at the maximum current densities, the resulting phosphor shows no color shift and low saturation.

Table 1. Composition of red-emitting CaS:Pb^{2+} , Mn^{2+} phosphor

| Materials | Mole (%) | By gram |
|------------------------|----------|---------|
| CaCO_3 | 100 | 100 |
| MnCO_3 | 0.5 | 0.575 |
| PbO | 0.3 | 0.670 |
| NH_4Cl | 2 | ~1 |

Table 2. Chemical elements in green-emitted CaS:Ce^{3+} phosphorus compound

| Materials | Mole (%) | By gram |
|-----------------|----------|---------|
| CaCO_3 | 100 | 100 |
| CeO_2 | 0.05 | 0.086 |

2.2. Simulation process

A simulated physical model utilized in the studies is shown in Figure 1(a), which includes nine blue chips, phosphor layers, and a dome-like lens. The precise measurements of this WLED are illustrated in Figure 1(b). The other figures of Figure 1 demonstrate WLED's four models packaged with different remote phosphor types: one-layer in Figure 1(c), two-layer with yellowish-red (YR), and yellow-green (YG) in Figures 1(d) and 1(e), respectively, and three-layer in Figure 1(f). The yellowish-emitting phosphor in the modeled packages is YAG:Ce^{3+} , and the substrate is aluminum nitride. The color correlated temperatures (CCTs) for packages are adjusted to 6600 and 7700 K which guarantee precision; moreover, all tests are performed across the vertical axis.

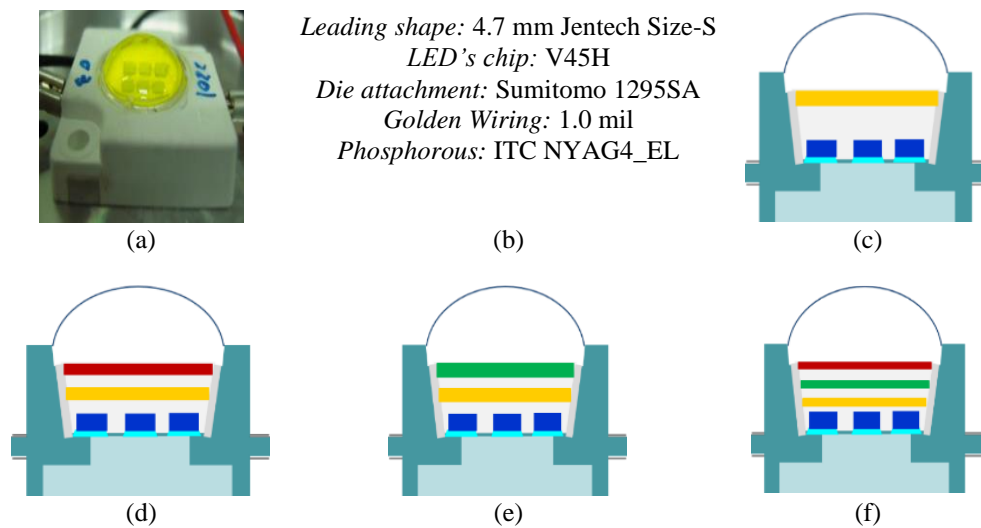


Figure 1. White LED multi-layer phosphor patterns (a) the representation of a real WLED, (b) WLED specifications, (c) one-layer remote phosphor (Y), (d) yellow-red two-layer remote phosphor (YR), (e) yellow-green two-layer remote phosphor (YG), and (f) three-layer remote phosphor

The distance between the remote phosphor films is set to 0.08 mm. The size parameter of phosphor grains used in this research is 14.5 μm . The adjustment of YAG:Ce^{3+} concentration responds to the changes in the green and red phosphors' concentrations for the consistency of the average CCTs. At each average CCT and in each phosphor structure, the YAG:Ce^{3+} concentration presents different values, resulting in variable lighting properties, which are caused by varying lighting effects of the scattering property in each WLED.

According to the content of Figure 2, Y structure (single-layer structure) has the highest yellow phosphor YAG:Ce³⁺ concentration. In contrast, the smallest concentration value of yellow phosphor is observed in the yellow-red-green triple-layer (YRG) configuration at both CCTs. Given that all the remote structures are examined at the same average color temperature, the more the YAG:Ce³⁺ concentration presents in the phosphor package, the greater the reabsorption losses, result in a reduction in luminous flux. Furthermore, the high concentration of YAG:Ce³⁺ causes an imbalance in the three colors including red, green, yellow that constitute white-emitted light, which is unfavored to WLED optical consistency.

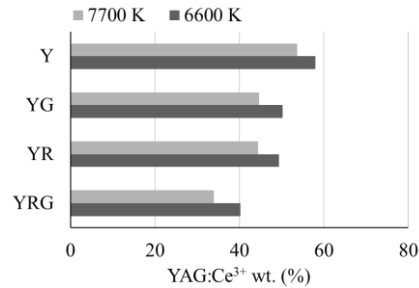


Figure 2. With different ACCTs values, yellow-emitted phosphor YAG:Ce³⁺ concentration correlating to specific phosphor structures

Stabilizing the equilibrium between the chromatic elements of white-light spectral band and stimulating the minimization of back-scattering light loss are the two most important factors for increasing the luminescent output and chromatic adequacy of WLEDs, as shown in Figure 3(a). The use of red-emission phosphors could help to achieve this goal since they provide red spectra to the spectral range of white lights, and thus boosting the ability of chromatic rendering of the LED package. On the other hand, the emission color of green from the green phosphor offers an overall control over the uniformity of color distribution and lumen intensity. The most favorable phosphor arrangement for increasing the illumination efficiency of WLEDs is the triple remote phosphor, which incorporates both red and green phosphor. However, we must take the emission spectrum of each remote phosphor model into consideration because it is another critical index that helps to comprehensively determine this argument. The diagrams of Figure 3(b) show the differences in the structures' emission spectra. When the width of the emission spectra is compared across all average color correlated temperatures (ACCTs), it is possible to claim that structure Y is the one yielding the lowest luminous efficiency because of its smallest emission spectra values. The three-layer YRG structure in contrast exhibits the highest spectral intensity in the 380-780 nm wavelength range. When comparing the two structures, we can see that YG configuration offers a higher luminous output in comparison to YR's one due to the YG's stronger spectral emission of the YG in the wavelength between 400 and 500 nm. However, in the range of wavelength from 650 to 700 nm, the intensity of emission spectra in YG is weaker than in the YR, which means that YR is preferable to chromatic rendering capabilities. The presented results are crucial clues to decide the best packaging design for WLED fabrication, but before reaching any conclusions, we must also evaluate part 3's findings.

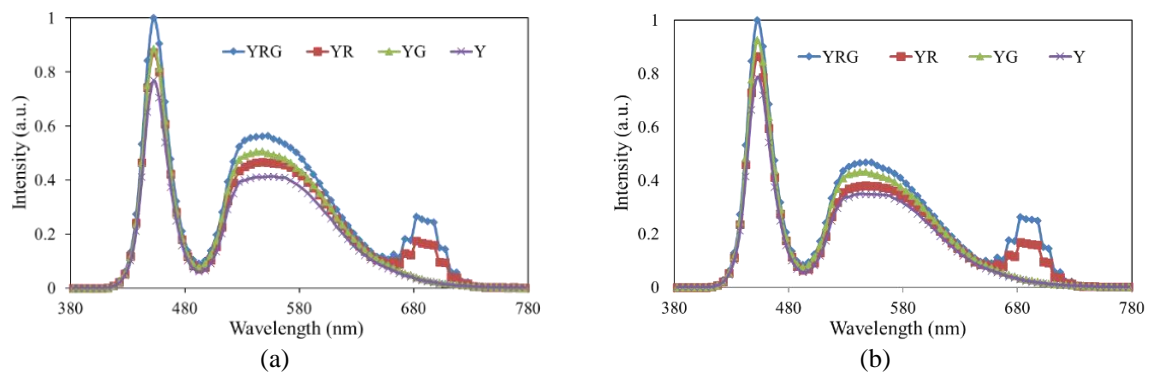


Figure 3. Emitting spectrum in four phosphorus models at (a) 6600 K and (b) 7700 K

3. RESULTS AND DISCUSSION

The evaluation of color performance of the four models in the study is first conducted with the color rendered indices. One of the most common parameters used for this aspect is color rendering index, shortened as CRI as shown in Figure 4. Also, from the graph, a significant finding regarding the rise of CRI is the increase of average CCTs can improve this parameter. Here, CRIs at 7700 K of all remote phosphor packages are higher than those at 6600 K. The graphs also reveal that the YR structure is the most conducive to CRI growth, with the greatest CRI of any ACCT. Despite the difficulty in monitoring the CRI of WLEDs above 7000 K CCTs, the YR structure can boost the CRI with the supplement of red components from red phosphor CaS:Pb^{2+} , Mn^{2+} . The YRG is second in terms of possible CRI, while the package of YG displayed the lowest CRI. These results imply that the YR structure is the most suitable for WLED fabrication to get excellent CRI improvement. Despite this, CRI can detect only a few aspects of a WLED's lighting qualities, but color quality scale (CQS), a broader and more difficult metric, can fully characterize a WLED's efficiency. The CQS has recently earned its popularity in the lighting research field and gradually become a crucial metric for light-color measurement owing to its integration of three main factors: CRI value, ocular choice of viewers, and color dimensions. This is a common metric for evaluating the WLEDs' chromatic output; the greater CQS, the more improved the color quality is. In Figure 5, this study expresses the calculated CQS of the simulated phosphor packaging constructions. The YRG shows the strongest CQS among the four examined simulations as this three-film phosphor design help balance the color distribution of three main chromatic elements: red, yellow, and green. Structure Y has the lowest CQS while having a larger luminous flux. In other words, its color quality cannot improve since it lacks red and green-emitted lights which are crucial factors in keeping the main colors balance to enhance the LED structure's chromatic performance. The chromaticity yielded from configuration Y is inferior to the others, but its simple manufacturing technique and inexpensive manufacturing cost make it a better alternative than other options.

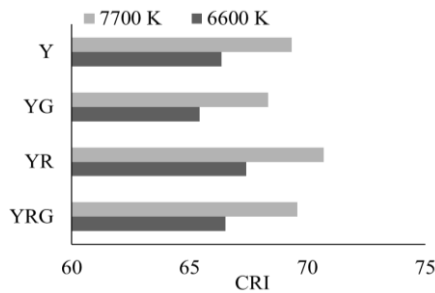


Figure 4. Color rendering indices of four phosphorus structures corresponding with average CCTs

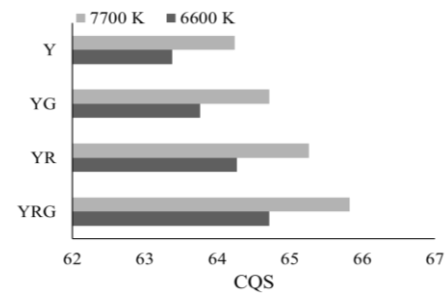


Figure 5. Four phosphorus structures' color quality scale corresponding with average CCTs

As indicated in Figure 5 result, if the production goal is the highest color improvement, it is appropriate to apply the YRG structure. So, for further evaluation on YRG performance, its luminous quality is investigated with support from the luminescence-efficiency comparison among the triple, dual and single-layer structures. The comparison is performed using the computation module and graphic illustration presented. The case of a dual-layer (DL) design in which h is the density for every phosphorus layer, the blue-conveyed light and yellow-transferred light are demonstrated by [27]–[29]:

$$PB_2 = PB_0 e^{-\alpha_{B_2} h} e^{-\alpha_{B_2} h} = PB_0 e^{-2\alpha_{B_2} h} \tag{1}$$

$$PY_2 = \frac{1}{2} \frac{\beta_2 PB_0}{\alpha_{B_2} - \alpha_{Y_2}} [e^{-\alpha_{Y_2} h} - e^{-\alpha_{B_2} h}] e^{-\alpha_{Y_2} h} + \frac{1}{2} \frac{\beta_2 PB_0}{\alpha_{B_2} - \alpha_{Y_2}} [e^{-\alpha_{Y_2} h} - e^{-\alpha_{B_2} h}]$$

$$= \frac{1}{2} \frac{\beta_2 PB_0}{\alpha_{B_2} - \alpha_{Y_2}} [e^{-2\alpha_{Y_1} h} - e^{-2\alpha_{B_1} h}] \tag{2}$$

In the meantime, each film of the phosphor in the triple-layer (TL) set up has a density of $\frac{2h}{3}$, and its the blue-conveyed light and yellow-transferred light may be presented using the calculation:

$$PB_3 = PB_0 \cdot e^{-\alpha_{B_2} \frac{2h}{3}} \cdot e^{-\alpha_{B_2} \frac{2h}{3}} \cdot e^{-\alpha_{B_2} \frac{2h}{3}} = PB_0 \cdot e^{-2\alpha_{B_3} h} \tag{3}$$

$$\begin{aligned}
 PY'_3 &= \frac{1}{2} \frac{\beta_3 PB_0}{\alpha_{B_3} - \alpha_{Y_3}} \left[e^{-\alpha_{Y_3} \frac{2h}{3}} - e^{-\alpha_{B_3} \frac{2h}{3}} \right] e^{-\alpha_{Y_3} \frac{2h}{3}} + \frac{1}{2} \frac{\beta_3 PB_0 e^{-\alpha_{B_3} \frac{2h}{3}}}{\alpha_{B_3} - \alpha_{Y_3}} \left[e^{-\alpha_{Y_3} \frac{2h}{3}} - e^{-\alpha_{B_3} \frac{2h}{3}} \right] \\
 &= \frac{1}{2} \frac{\beta_3 PB_0}{\alpha_{B_3} - \alpha_{Y_3}} \left[e^{-\alpha_{Y_3} \frac{4h}{3}} - e^{-2\alpha_{B_3} \frac{4h}{3}} \right]
 \end{aligned} \tag{4}$$

$$\begin{aligned}
 PY_3 &= PY'_3 \cdot e^{-\alpha_{Y_3} \frac{2h}{3}} + PB_0 \cdot e^{-2\alpha_{B_3} \frac{4h}{3}} \frac{1}{2} \frac{\beta_3}{\alpha_{B_3} - \alpha_{Y_3}} \left[e^{-\alpha_{Y_3} \frac{2h}{3}} - e^{-\alpha_{B_3} \frac{2h}{3}} \right] \\
 &= \frac{1}{2} \frac{\beta_3 PB_0}{\alpha_{B_3} - \alpha_{Y_3}} \left[e^{-\alpha_{Y_3} \frac{4h}{3}} - e^{-\alpha_{B_3} \frac{4h}{3}} \right] e^{-\alpha_{Y_3} \frac{2h}{3}} + \frac{1}{2} \frac{\beta_3 PB_0 e^{-\alpha_{B_3} \frac{4h}{3}}}{\alpha_{B_3} - \alpha_{Y_3}} \left[e^{-\alpha_{Y_3} \frac{2h}{3}} - e^{-\alpha_{B_3} \frac{2h}{3}} \right] \\
 &= \frac{1}{2} \frac{\beta_3 PB_0}{\alpha_{B_3} - \alpha_{Y_3}} \left[e^{-\alpha_{Y_3} h} - e^{-2\alpha_{B_3} h} \right]
 \end{aligned} \tag{5}$$

The denseness of every phosphorus sheet within remote phosphor packages is indicated by h in the preceding calculations. In addition, the DL and TL configurations are correlatively represented by the subscripts “2” and “3”. The converted coefficient of blue-emitted light shifting to yellow is represented by β , whereas the yellow-emitted light radiation patterns is denoted by γ . Blue-emitted light (PB) with yellow-emitted light (PY) intensities are blue LEDs’ light intensities, which are depicted as PB_0 . B and Y are the amounts of power dissipated of blue and yellow-colored photons as they spread through the phosphorus layer. Furthermore, the yellow light transmitted via two phosphor layers is represented as PY'_3 in (4). Using the triple-layer remote phosphor configuration considerably improves the lighting performance of a WLED products, which is much greater compared to the light output of the dual-layer design:

$$\frac{(PB_3 - PY_3) - (PB_2 + PY_2)}{(PB_2 + PY_2)} > \frac{e^{-2\alpha_{B_3} h} - e^{-2\alpha_{B_2} h}}{e^{-2\alpha_{Y_3} h} - e^{-2\alpha_{B_2} h}} > 0 \tag{6}$$

The equation (6) demonstrates that using three phosphor layers instead of two layers improves the luminous flux. Figure 6 shows the luminous efficacy (LE) of all four simulated configurations, revealing that the YRG outperforms the Y structure in all ACCTs. This demonstrated that the YRG structure, in addition to having the best color efficiency, also has the most luminous flux. The presence of not only green phosphor but also red phosphor materials in the remote phosphor package of the structure YRG causes the yellow YAG:Ce³⁺ concentration to considerably decrease, and consequently reducing the back-scattering and re-absorption events leading to light loss. As the YAG:Ce³⁺ amount falls, the performance in power conversion improves owing to the higher transmission efficiency of LED chip-emitting blue lights. In other words, the degradation of yellow-phosphor concentration helps the blue lights easily get through the yellow phosphor film to contact with other layers in the package. As a consequence, in comparison with the other configurations, the intensity of the emission spectrum within white-emitting light wavelength values, with YRG system luminescent output are at peak. Furthermore, the supplemented green-light components from the green CaS:Ce³⁺ film enhances the emission spectrum of the YG structure within 500 to 600 nm wavelength band, rendering it better than either the YR structure or the Y model. As a result, the YG structure has the second-highest luminous flux.

The demonstrated benefits of YRG package make it a great solution to give WLED great lighting consistency in CQS and LE. Furthermore, while discussing color quality, color homogeneity is critical. Even though the scattering-enhancement particles and the conformal coating method are the two most preferred approaches for boosting color uniformity, they can significantly diminish the light flux of WLEDs. Thus, the solution is to use the red CaS:Pb²⁺, Mn²⁺ and green CaS:Ce³⁺ phosphors with the remote phosphor structural design. The phosphor layers can stimulate not only the scattering efficiency but also quality of white-light output, while the structural design of remote phosphor layer offers great capability to reduce the internal light reflection and circulation, resulting in enhanced light extraction and luminous output. In contrast, according to (6), the concentration of each phosphor layer needed to be adjusted precisely to achieve the best energy transmission efficiency. Figure 7 depicts the chromatic differences among four remote-layer WLED packages. The lowest color deviation (D-CCT) leads to the highest color homogeneity, and thus in this figure, the configuration YRG has the best performance in chromaticity regarding its smallest color deviation. This can be because of the enhancement of scattering occurrences within the YRG-LED package, allowing the multiplication of light mixing process to be performed before generating white light. As a result, the increased color uniformity is recognized. Yet, if there are too many scattering occurrences, the luminous efficacy will be diminished. However, the reduction of the back-scattering effect compensates for this disadvantage. Hence, YRG model maintains the maximum chromatic homogeneity while exhibiting the highest luminescent output, compared to the other structuring figures. Conversely, structure Y has the largest color variance measurement of any average CCT.

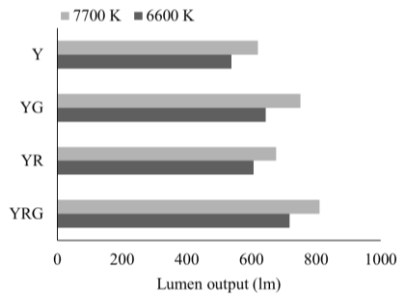


Figure 6. Lumen output of four phosphorus structures emulating the average CCTs

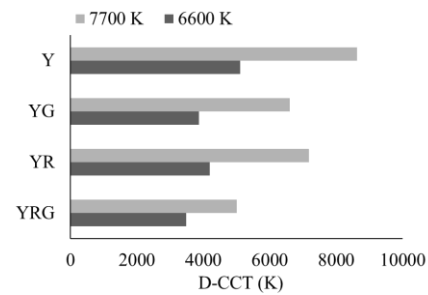


Figure 7. Correlating color diversity (D-CCT) in four phosphorus structures emulating the average CCTs

4. CONCLUSION

In summary, the YRG is the ideal remote phosphor structure for WLEDs because it provides a chromatic balance for the three-color distribution, significant reduction in back-scattering light loss, and the smallest color difference, which results in the best luminous flux, color quality, and color uniformity. Furthermore, when comparing the two dual-layer structures, the YG exhibits stronger flux intensity and better uniformity of white-light color than the YR performs. After all, the added green spectral elements from the layer of green phosphor $\text{CaS}:\text{Ce}^{3+}$ improves luminescence efficiency as well as color homogeneity, while YR configuration has better values of both CRI, CQS because the red light component is advantageous for CRI and CQS. These are the results of a quantitative experiment comparing the optical properties of Y, YG, YR, and YRG structures, which were conducted in this study and confirmed based on the Mie hypothesis with Lambert-Beer basis. The information from this paper can serve as a valuable reference for manufacturers to choose the optimal structure for producing high-quality WLEDs.

ACKNOWLEDGEMENTS

This research is supported by Industrial University of Ho Chi Minh City (IUH) under grant number 121/HD-DHCN.




REFERENCES

- [1] S. Lee, Y. Kim, and J. Kim, "Solution-processed NiO as a hole injection layer for stable quantum dot light-emitting diodes," *Applied Sciences*, vol. 11, no. 10, May 2021, doi: 10.3390/app11104422.
- [2] K. J. Noh, J. Choi, J. S. Hong, and K. R. Park, "Finger-vein recognition using heterogeneous databases by domain adaption based on a cycle-consistent adversarial network," *Sensors*, vol. 21, no. 2, Jan. 2021, doi: 10.3390/s21020524.
- [3] F. Arena and G. Pau, "An overview of big data analysis," *Bulletin of Electrical Engineering and Informatics (BEEI)*, vol. 9, no. 4, pp. 1646–1653, Aug. 2020, doi: 10.11591/eei.v9i4.2359.
- [4] Y. Chu *et al.*, "Perception enhancement using importance-driven hybrid rendering for augmented reality based endoscopic surgical navigation," *Biomedical Optics Express*, vol. 9, no. 11, pp. 5205–5226, Nov. 2018, doi: 10.1364/BOE.9.005205.
- [5] L. Duan and Z. Lei, "Wide color gamut display with white and emerald backlighting," *Applied Optics*, vol. 57, no. 6, pp. 1338–1344, Feb. 2018, doi: 10.1364/AO.57.001338.
- [6] Y. Peng *et al.*, "Flexible fabrication of a patterned red phosphor layer on a $\text{YAG}:\text{Ce}^{3+}$ phosphor-in-glass for high-power WLEDs," *Optical Materials Express*, vol. 8, no. 3, pp. 605–614, Mar. 2018, doi: 10.1364/OME.8.000605.
- [7] X. Li *et al.*, "Highly stable and tunable white luminescence from Ag-Eu^{3+} co-doped fluoroborate glass phosphors combined with violet LED," *Optics Express*, vol. 26, no. 2, pp. 1870–1881, Jan. 2018, doi: 10.1364/OE.26.001870.
- [8] J. Lui, A. M. Vegni, L. Colace, A. Neri, and C. Menon, "Preliminary design and characterization of a low-cost and low-power visible light positioning system," *Applied Optics*, vol. 58, no. 26, pp. 7181–7188, Sep. 2019, doi: 10.1364/AO.58.007181.
- [9] Z. Zhou, G. Liu, J. Ni, W. Liu, and Q. Liu, "White light obtainment via tricolor luminescent centers and energy transfer in $\text{Ca}_3\text{ZrSi}_2\text{O}_9:\text{Eu}^{3+}, \text{Bi}^{3+}, \text{Tb}^{3+}$ phosphors," *Optical Materials Express*, vol. 8, no. 11, Nov. 2018, doi: 10.1364/OME.8.003526.
- [10] B. Wang, D. S. Li, L. F. Shen, E. Y. B. Pun, and H. Lin, " Eu^{3+} doped high-brightness fluorophosphate laser-driven glass phosphors," *Optical Materials Express*, vol. 9, no. 4, pp. 1749–1762, Apr. 2019, doi: 10.1364/OME.9.001749.
- [11] Y. Li *et al.*, "395 nm GaN-based near-ultraviolet light-emitting diodes on Si substrates with a high wall-plug efficiency of 520%@350 mA," *Optics Express*, vol. 27, no. 5, pp. 7447–7457, Mar. 2019, doi: 10.1364/OE.27.007447.
- [12] S. An, J. Zhang, and L. Zhao, "Optical thermometry based on upconversion luminescence of $\text{Yb}^{3+}\text{-Er}^{3+}$ and $\text{Yb}^{3+}\text{-Ho}^{3+}$ doped Y_6WO_{12} phosphors," *Applied Optics*, vol. 58, no. 27, pp. 7451–7457, Sep. 2019.
- [13] K. Matsuhashima and N. Sonobe, "Full-color digitized holography for large-scale holographic 3D imaging of physical and nonphysical objects," *Applied Optics*, vol. 57, no. 1, pp. A150–A156, Jan. 2018, doi: 10.1364/AO.57.00A150.
- [14] J. Ji, G. Zhang, S. Yang, X. Zhang, X. Zhang, and C. C. Yang, "Theoretical analysis of a white-light LED array based on a GaN nanorod structure," *Applied Optics*, vol. 59, no. 8, pp. 2345–2351, Mar. 2020, doi: 10.1364/AO.387059.
- [15] V. Dumont, S. Bernard, C. Reinhardt, A. Kato, M. Ruf, and J. C. Sankey, "Flexure-tuned membrane-at-the-edge optomechanical system," *Optics Express*, vol. 27, no. 18, pp. 25731–25748, Sep. 2019, doi: 10.1364/OE.27.025731.
- [16] S. Kumar, M. Mahadevappa, and P. K. Dutta, "Extended light-source-based lensless microscopy using constrained and




- regularized reconstruction,” *Applied Optics*, vol. 58, no. 3, pp. 509–516, Jan. 2019, doi: 10.1364/AO.58.000509.
- [17] S.-R. Chung, C.-B. Siao, and K.-W. Wang, “Full color display fabricated by CdSe bi-color quantum dots-based white light-emitting diodes,” *Optical Materials Express*, vol. 8, no. 9, pp. 2677–2686, Sep. 2018, doi: 10.1364/OME.8.002677.
- [18] A. Neitz *et al.*, “Effect of cone spectral topography on chromatic detection sensitivity,” *Journal of the Optical Society of America A*, vol. 37, no. 4, pp. A244–A254, Apr. 2020, doi: 10.1364/JOSAA.382384.
- [19] L. Li *et al.*, ““Roller coaster”-like thermal evolution of the Er³⁺ ion’s red photoluminescence in CaWO₄:Yb³⁺/Er³⁺ phosphors,” *Optics Letters*, vol. 44, no. 17, Sep. 2019, doi: 10.1364/OL.44.004411.
- [20] S. Cincotta, C. He, A. Neild, and J. Armstrong, “High angular resolution visible light positioning using a quadrant photodiode angular diversity aperture receiver (QADA),” *Optics Express*, vol. 26, no. 7, pp. 9230–9242, Apr. 2018, doi: 10.1364/OE.26.009230.
- [21] Z. Zhao, H. Zhang, S. Liu, and X. Wang, “Effective freeform TIR lens designed for LEDs with high angular color uniformity,” *Applied Optics*, vol. 57, no. 15, pp. 4216–4221, May 2018, doi: 10.1364/AO.57.004216.
- [22] J. Li, Y. Tang, Z. Li, X. Ding, L. Rao, and B. Yu, “Investigation of stability and optical performance of quantum-dot-based LEDs with methyl-terminated-PDMS-based liquid-type packaging structure,” *Optics Letters*, vol. 44, no. 1, pp. 90–93, Jan. 2019, doi: 10.1364/OL.44.000090.
- [23] C. J. C. Smyth, S. Mirkhanov, A. H. Quarterman, and K. G. Wilcox, “275 W/m² collection efficiency solar laser using a diffuse scattering cooling liquid,” *Applied Optics*, vol. 57, no. 15, May 2018, doi: 10.1364/AO.57.004008.
- [24] B. Qiu, K. Li, and X. Li, “Synthesis and enhanced luminescent properties of SiO₂@LaPO₄:Ce³⁺/Tb³⁺ microspheres,” *Optical Materials Express*, vol. 8, no. 1, pp. 59–65, Jan. 2018, doi: 10.1364/OME.8.000059.
- [25] H.-Y. Yu *et al.*, “Solar spectrum matching with white OLED and monochromatic LEDs,” *Applied Optics*, vol. 57, no. 10, pp. 2659–2666, Apr. 2018, doi: 10.1364/AO.57.002659.
- [26] Y. Yu *et al.*, “Improving the color-rendering index of a tandem warm white organic light-emitting device by employing a simple fabrication process,” *Optics Letters*, vol. 44, no. 4, pp. 931–934, Feb. 2019, doi: 10.1364/OL.44.000931.
- [27] L. M. Lozano *et al.*, “Optical engineering of polymer materials and composites for simultaneous color and thermal management,” *Optical Materials Express*, vol. 9, no. 5, pp. 1990–2005, May 2019, doi: 10.1364/OME.9.001990.
- [28] Y. Zhang, X. Zhu, A. Liu, Y. Weng, Z. Shen, and B. Wang, “Modeling and optimizing the chromatic holographic waveguide display system,” *Applied Optics*, vol. 58, no. 34, pp. G84–G90, Dec. 2019, doi: 10.1364/AO.58.000G84.
- [29] W. Gao, K. Ding, G. He, and P. Zhong, “Color temperature tunable phosphor-coated white LEDs with excellent photometric and colorimetric performances,” *Applied Optics*, vol. 57, no. 31, pp. 9322–9327, Nov. 2018, doi: 10.1364/AO.57.009322.

BIOGRAPHIES OF AUTHORS






Dieu An Nguyen Thi    received a master of Electrical Engineering, HCMC University of Technology and Education, Vietnam. Currently, she is a lecturer at the Faculty of Electrical Engineering Technology, Industrial University of Ho Chi Minh City, Viet Nam. Her research interests are Theoretical Physics and Mathematical Physics. She can be contacted at email: nguyenthidieuan@iuh.edu.vn.



My Hanh Nguyen Thi    received a Bachelor of Physics from An Giang University, Viet Nam, Master of Theoretical Physics And Mathematical Physics, Hanoi National University of Education, Vietnam. Currently, she is a lecturer at the Faculty of Mechanical Engineering, Industrial University of Ho Chi Minh City, Viet Nam. Her research interests are Theoretical Physics and Mathematical Physics. She can be contacted at email: nguyenthimyhanh@iuh.edu.vn.



Phuc Dang Huu    received a Physics Ph.D. degree from the University of Science, Ho Chi Minh City, in 2018. Currently, He is Research Institute of Applied Technology, Thu Dau Mot University, Binh Duong Province, Vietnam. His research interests include simulation LEDs material, renewable energy. He can be contacted at email: danghuuphuc@tdmu.edu.vn.